*Table of contents*

# Environment / Climate / Naural Hazards / Simulation

*Environment / Climate / Naural Hazards / Simulation*

# Mathematical Tools for Modeling Natural Risks

MAXIMILIAN F. HASLER

*D.S.I., Laboratoire A.O.C., Université des Antilles et de la Guyane, B.P. 7209, F-97275 SCHOELCHER cedex, Martinique (F.W.I.), France - Maximilian.Hasler@martinique.univ-ag.fr*

**Abstract**

Without attempting to give a complete overview of the rich knowledge existing in the field addressed by the title, we discuss several recent original and powerful, but not always very well known mathematical tools, which find their application in mathematical models of natural risks, with special emphasis on the description of singularities and their propagation, in particular in the context of shock waves, hurricanes and tsunami. We consider two categories of these tools: on one hand, theories from functional analysis designed to find solutions to partial differential equations with singularities of various types, and on the other hand, numerical methods which are useful when these models are applied in concrete calculations. As an illustration, we present an interesting mathematical model for the prediction of hurricane tracks.

## Introduction

Through the past years, the need for precise mathematical models, describing natural phenomena potentially constituting a hazard for population and/or environment accurately enough to allow reliable predictions, has proved more and more evident. These models are usually made from three basic building blocks: heuristics based on experience, rigorous theory, and numerical calculations. The first leads to a system of equations reasonably well describing the phenomena, the second is necessary to ensure that manipulation of these equations will not introduce new (unrealistic) or exclude relevant existing solutions, and the third will allow to apply the model to reality, which usually requires treatment of a large amount of data in order to yield a realistic description. In this paper, we will discuss in how far these issues, in particular the second one, need to be reconsidered in the context we are interested in, where "classical" ideas, theories and well-established techniques become inadequate or even invalid.

## Mathematical aspects of catastrophes

The violence of phenomena related to natural risks corresponds from a mathematical point of view to *singularities* of the functions describing the physical system. These range from insufficient smoothness through functions having jumps in their graph, up to objects which are so "rough" that they can no more be considered as functions in the usual sense. Still, they can be rigorously described and manipulated in the mathematical theory of Schwartz distributions, as long as only linear operations are involved.
Physical laws, especially equations of motion, usually involve differential operators that tend to increase irregularities of the initial data. However, if the latter are sufficiently smooth, irregularities will not be appear "out of nothing", as long as the laws respectively the associated operators remain *linear*.

## Non-linearity as source of singularities

The key property responsible for the birth of natural catastrophes is thus the *non-linearity* of the physical laws describing these phenomena. This can be illustrated by considering Burger's equation

$$\partial_t u + u\, \partial_x u = 0$$

which can be seen as a simplified version of the more realistic Navier-Stokes equation from fluid dynamics we use later for modeling hurricanes. The presence of the non-linear term $u\ \partial_x\ u$ makes it impossible to treat this quite simple wave equation in the framework of Schwartz distributions (which cannot be multiplied among themselves). A solution to this equation, for initial data $u(0,x) = u_0(x)$, is given by

$$u(t,x) = u_0(x - t\, u(t,x)) = u_0(y) \quad \text{for} \quad x = y + t\, u_0(y)\ .$$

It is easy to see that a point (x, $u_0(x)$) will propagate to the left with speed $u_0(x)$. Thus, the negative slope to the right of a maximum of $u_0$ will tend to $-\infty$ in a finite time: a shock wave is born out of smooth initial data!

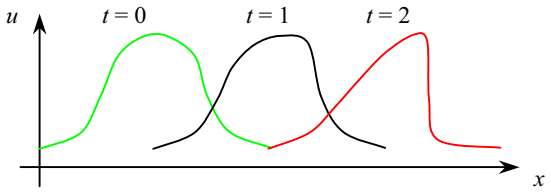


Fig. 1: formation of a shock wave from smooth initial data in Burger's nonlinear wave equation

## Algebras of generalized functions

Since non-linearity and singularities are characteristic ingredients in realistic descriptions of natural risks, but the two cannot be combined in the classical theory, one needs (new) generalized functions which form *algebras*, i.e. which can be multiplied among themselves. Such a theory has been proposed by Colombeau in the 1980s, and has since then seen important developments, especially during the last decade. The idea is to take quotient spaces $G = E_M / E_N$ of "moderate" modulo "negligible" sequences of functions, where these properties refer to growth with respect to some regularization parameter ε. For example, $E_M$ may contain sequences $(f_\varepsilon)_\varepsilon$ growing like *some* power $\varepsilon^{-p}$ when $\varepsilon \to 0$, while the $(f_\varepsilon)_\varepsilon \in E_N$ will decrease to 0 faster than *any* power $\varepsilon^p$. The value of such generalized functions in a point are *generalized numbers*, which can represent "infinite" quantities in a precise manner.

**Application: soliton waves**

If we add an "infinitesimally small" term $[\varepsilon]\ \partial_x^3\ u$ to Burger's equation, where [ε] is a generalized number associated (i.e. in the "classical" limit equal) to zero, we get the Korteweg-deVries equation with small dispersion. It has as an exact solution the function

$$u(t,x) = 3\ c\ \cosh^{-2}(\ b\ (\ x - c\ t\ -\ x_0\ )/2)$$

for arbitrary (generalized!) numbers $b$ and $x_0$, which represents a soliton wave moving with speed $c = [\varepsilon]\ b^2$ to the left. If $b$ is a finite number, then the speed and the amplitude of the wave are infinitesimally small. But the speed can also be finite; then $b$ is a infinitely large number, which means that classically the wave is zero in any point except $x_0 + c\ t$, where it has a finite value. In usual distribution theory, this object cannot be distinguished from the zero function. However, the derivative of $u$ (which is related to the energy transported by the wave) is not bounded; it corresponds to the difference of two δ-distributions located at $x_0 + c\ t \pm \ln(2+\sqrt{3})/b$. One can also consider the case of a finite overall "mass" $\int\ u(x,t)\ dx = 12\ c/b = 12\ [\varepsilon]\ b$. Then the solution resembles to a δ-distribution moving with infinite speed, since $c$ and $b$ are both infinitely large.

**Asymptotic expansions**

A quite different approach from Colombeau's theory, which can also yield a differential algebra of generalized functions, is that of asymptotic expansions. Here one considers a collection of particular (non-smooth) generalized functions, which can be multiplied by smooth functions. According to the application, this collection might contain the Dirac distribution, and power series in a regularization parameter ε. In the sequel we describe a variant of this which has been used to develop a model for the prediction of hurricane tracks.
While shock waves, whose support is a hyperplane, have been studied since a long time, but only in the 1980s V.P. Maslov and collaborators started to study propagation of structurally stable *weak* singularities having a support of codimension > 1; examples have then been constructed in the setting of asymptotic expansions.

**Application: dynamics of the hurricane's eye**

The hurricane's eye is the typical example of a point-like weak singularity propagating in $D \geq 2$ dimensions. It can be described as follows: Starting from the full Navier-Stokes equations and conservation of mass,

$$\rho\ (\partial_t\ \mathbf{u} + \mathbf{u}\cdot\nabla\ \mathbf{u}) = -\nabla\ p + \eta\ \Delta\ \mathbf{u}\ ,\ \ \partial_t\ \rho + \mathrm{div}(\rho\ \mathbf{u}) = 0\ ,$$

which describes the flow $\mathbf{u}$ of a fluid with density ρ, pressure $p$, and viscosity η, we go into a coordinate system relative to a point $X(t)$, taken to be the position of the eye on the earth's surface, to which we restrict the dynamics, and whose rotation introduces Coriolis' acceleration $\mathbf{a}_C = 2\ \mathbf{u} \times \mathbf{\Omega}$ (depending on the latitude):

$$\rho\ (\partial_t\ \mathbf{U} + \mathbf{X''} + \mathbf{U}\cdot\nabla\ \mathbf{U} + 2\ (\mathbf{U} + \mathbf{X'}) \times \boldsymbol{\omega}\ ) = -\nabla\ p + \eta\ \Delta\ \mathbf{U}\ .$$

In this two dimensional approximation, the pressure is replaced by a function of the density, $p = k\ \rho^{2+\delta}$. Taking $\eta = 0$, one gets the so-called shallow water equations. Neglecting viscosity seems reasonable for air, but we keep in mind the big gradients of $\mathbf{u}$ expected near the eye, and that this term improves stability of the equations.

**Decomposition into regular and singular part**

Following seminal work by V. N. Zhikharev, we consider solutions of which each component is of the form

$$f(x) = f^0(x) + S(x)\ f^1(x)\ ,$$

where $f^0$ and $f^1$ are smooth functions, while $S$ presents a weak singularity in one point (which will be the hurricane's position). Theoretical considerations by Zikharev, Maslov and others imply that $S(x)$ must be of the form $S(x) = \beta(x - X_0)^{1/2}$, where β is a positive quadratic form. This has as a consequence that the product of such functions will again be of the same type. We try to find solutions of this form to the above equations, which means that the density $\rho(t,x)$ and each of the three components of the flow $\mathbf{u}(t,x)$ are decomposed into a smooth part $(\rho^0, \mathbf{u}^0)$ and a "singular" part $(\rho^1,\mathbf{u}^1)$ which multiplies $S(x)$. One then finds that the equations allow themselves also for such a decomposition in a smooth and a singular part, symbolically

$$E(\rho,u) = 0 \quad \Leftrightarrow \quad E^0(\rho,u) + S\ E^1(\rho,u) = 0\ ,$$

while both parts involve as well the smooth as the singular components of the unknown functions.

The next crucial step is to show that these two parts of the equations can be considered independently. In fact, this is justified in an immediate neighborhood of the point $X(t)$ where the singularity is located. Roughly speaking, since the function $S(x)$ does not allow an asymptotic expansion around $x = X(t)$, the Taylor coefficients of the regular and singular part can be identified separately, order by order.

**Truncation of the chain**

By doing so, we obtain an *infinite* chain of equations for the Taylor coefficients $(\rho_{ij},\mathbf{u}_{ij})^{0,1}$, which are functions of time only. Thus, the system of PDE's has been reduced to a sequence of *ordinary* differential equations. Analyzing them order by order shows that many of the equations turn out to be purely algebraic, in virtue of preceding results. These allow to express "directly" some unknown components in terms of other ones. Of course, an infinite number of equations cannot be dealt with, so one must proceed to a truncation of the chain at some order. A thorough study concerning this truncation has been done for the model under investigation, but there still remain open theoretical questions concerning the general case of such developments. Using the computer algebra system Maple, we have pushed the calculation to include all terms up to the third order, while previous work only considered terms up to the second order. We also made all calculations for nonzero values of η and the parameter δ, which seems strongly motivated by phenomenological laws of state.

**Numerical optimization**

Now we are able to determine the trajectory $\mathbf{X}(t)$ of the singularity (among other information) by simply integrating the system of ODE's, for given initial data. However, the "correct" values of the latter are not directly known. We wish to determine the important number of these unknown initial data $\xi$ for the coefficient functions, in such a way that the integral curve $\mathbf{X}(t;\xi)$ of the eye's track matches as well as possible a given collection $\{ \mathbf{X}(t_i) \}$ of already available measured points. Then we can assume that extrapolation to future times will give a reasonably good prediction of the track. Minimizing the error

$$E(\xi) = \sum_i \rho(t_i) \, \| \mathbf{X}(t_i;\xi) - \mathbf{X}(t_i) \|^2$$

(where $\rho$ is a weight function) requires an efficient method of high-dimensional numerical optimization.

This takes us to another general and frequent problem arising in mathematical models of the reality, which nearly always involve a process of fitting parameters which cannot be determined from theory, to get a "best approximation". To find a sequence $(\xi_k)$ converging to the optimal value $\xi^*$, we choose step by step a direction $\mathbf{d}_k$ and then perform a *linear search* to determine $\boldsymbol{\delta}_k = \alpha_k \, \mathbf{d}_k = \xi_{k+1} - \xi_k$ minimizing $E(\xi_{k+1})$.
The most naïve *steepest decent* method $\mathbf{d}_k = -\nabla E(\xi_k)$ is easily seen to be a bad choice in general, but also the rapidly converging *Newton's method* $\mathbf{d}_k = - \mathrm{B}(\xi_k) \, \nabla E(\xi_k)$, where B is the inverse matrix of the Hessian $\mathrm{H} = \mathrm{D}^2 E$, is inadequate since the calculation of H requires about $n^2$ evaluations of $E$ (involving in our case numerical integration of $n = 15$ or 30 ODE's to calculate each $\mathbf{X}(t_i;\xi)$!), plus $\mathrm{O}(n^3)$ operations for the matrix inversion. This is avoided by *quasi-Newton methods*, where $\mathrm{B}(\xi_k)$ is replaced by an approximation $\mathrm{B}_k$ which can be calculated at low cost. The improved Broyden-Fletcher-Goldfarb-Shanno (BFGS) formula,

$$\mathrm{B}_{k+1} = \mathrm{B}_k + \gamma \, [(1 + \gamma \, \mathbf{y} \cdot \mathbf{b}) \, \boldsymbol{\delta}\boldsymbol{\delta}^{\mathrm{T}} - \mathbf{b}\boldsymbol{\delta}^{\mathrm{T}} - \boldsymbol{\delta}\mathbf{b}^{\mathrm{T}}],$$

where $\mathbf{y} = \nabla E(\xi_{k+1}) - \nabla E(\xi_k)$, $\mathbf{b} = \mathrm{B}_k \cdot \mathbf{y}^{\mathrm{T}}$, $\gamma = 1/\mathbf{y} \cdot \boldsymbol{\delta}$, is one of the most efficient implementations of this idea, avoiding any matrix inversion. Combined with heuristic rules for inexact line search (Armijo's rule, Wolfe conditions) this yields a very efficient all-purpose minimizing routine, which we tuned for our purpose by adding additional stopping criteria, among others for early detection of approaching irrelevant parameter domains. For numerical integration, we chose classical $4^{\text{th}}$-$5^{\text{th}}$ order Runge-Kutta routines, and sped up the (vector valued) function evaluation by methods of automatic code optimization, e.g. with respect to common subexpressions.

**Discussion of results**

Once the optimization procedure is "connected" to the function $\mathbf{X}(t;\xi)$ which corresponds to the numerical integration of the truncated chain of ODE's, we can predict, i.e. extrapolate a given trajectory to future times. A basic version of this model had already been proposed over 10 years ago. In spite of its simplicity, it already gave quite satisfactory predictions in generic situations. Using computer algebra systems, we could take into account the next order in the Hugoniot-Maslov chain and nonzero values for $\eta$ and $\delta$. This considerably complicates the (theoretical) calculations, but yields better numerical stability and a more realistic model, allowing finally even better long-term predictions than the already promising original model. However, new conceptual challenges arise with this extended model, for example concerning the choice of the starting point for the optimization procedure.

One of the important features of the model is the relatively low cost in calculation power, compared to traditional finite element methods, which still persists even if the equations become more complicated as the model gets refined. Another advantage lies in the fact that it can not only predict the hurricane's track, but also other relevant information, e.g. estimates for the wind strength near the hurricane's eye, and even information on *gradients* of data like the density of air.
Of course, the model can and should be refined in several ways to become more accurate from the phenomenological point of view. It could for example take into account external factors like the ocean's surface temperature (crucial for the hurricane's dynamics), geographical data, etc. Another improvement would be to use a multi–layer model, to take into account the different physical conditions, in particular temperature, at higher altitudes. Anyway, it should be obvious that this is more than just a toy model, and clearly deserves to be studied further.

However, the presentation of this model was not the only purpose of this paper. It rather served as a nice and interesting illustration of how recent theoretical advances from quite different domains come to a productive interplay in the context of nonlinear differential problems, which are typical for models describing natural risks, and where many well established classical methods can no more be used. This area of research is challenging for both practical and theoretical motivations. The former are evident, and concerning the latter, we hope that we could give enough insight into the generically new problems arising here, but also on the quite powerful recently developed tools which may used to tackle these problems, particularly relevant in our geographical context.

**References**

1. J.-F. Colombeau (1984), New generalized functions and multiplication of distributions, North Holland.
   A. Delcroix, M. F. Hasler, S. Pilipović and V. Valmorin (2004), *Proc. Amer. Math. Soc.* **132**:2031.
2. V. Butalov, Yu. Vladimirov, V. Danilov and S. Dobrokotov (1994), *Mathematical Notes* **55**(3):11.
   S. Yu. Dobrokhotov, K. V. Pankrashkin and E. S. Semenov (2001), *Russian J. of Math. Physics* **8**(1):25.
   S. Yu. Dobrokhotov, E. S. Semenov, B. Tirozzi (2004), *Theoretical & Mathematical Physics* **139**(1): 500.
   V. P. Maslov (1980), *Russ. Math. Surv.* **35**(2):252.
   V. N. Zhikharev (1986), Dep. VINITI, No. 8148-B86, Moscow.
3. C. G. Broyden (1970), *J. Inst. Math. Comput.* **6**:222.
   R. Fletcher (1970), *Comput. J.* **13**:317.
   D. Goldfarb (1970), *Math. Comput.* **24**:23.
   D.F. Shanno (1970), *Math. Comput.* **24**:647.
   H.Y. Huang (1970), *J. Opt. Theor. Applic.* **5**:405.
   J.C. Gilbert, C. Maréchal (1989), *Math. Progr.* **45**:407.
   W. H. Press, S. Teukolsky, W. Vetterling, B.P. Flannery (1992), Numerical recipes in C, Camb. Univ. Press.
   R. H. Byrd, P. Lu, J. Nocedal, C. Zhu (1995), *SIAM J. Sci. Comp.* **16**(5):1190.

*Environment / Climate / Natural Hazards / Simulation*

# Climatological Analysis of Deep Convective Days in Guadeloupe

N. NATHOU, E. HICKS

*Laboratoire de Physique de l'Atmosphère Tropicale, Université des Antilles et de la Guyane*
*BP 250, 97157 Pointe-à-Pitre Cedex, nnathou@univ-ag.fr*

**Abstract**

The satellite lightning observations (LIS and OTD) clearly show a marked contrast between lightning activity over land and ocean. Two hypotheses have been formulated to explain the physical origin of this contrast: the thermal and the aerosol hypothesis. In this study, a climatological analysis on thunderstorm days over a period of 33 years has been carried out in order to test the role of the surface temperature on cloud electrification as supposed by the thermal hypothesis. In a second time, the dynamical characteristics (maximum cloud top height, vertical velocity, CAPE and CIN) in both the storm and deep convective clouds have been compared by using a 1D cloud model, initialized with the corresponding appropriate atmospheric sounding. According to the results, the clouds that have been observed on days with deep convection have dynamical characteristics as on storm days, but have not developed any significant electricity leading to lightning.

## Introduction

The lightning production of thunderstorm clouds is of interest in different fields of research, engineering and civil protection. However, the mechanisms which govern the global atmospheric electrical circuit remain still badly known. This ignorance delays the development of certain applications such as reflection, refraction and diffusion of the radio waves by the ionized layers of the upper atmosphere among which telecommunications hold a significant part. Tropospheric storms are electric generators of current which bring electricity in altitude through the conductive atmosphere. Lightning discharges play a key role in the maintenance of the ionosphere to a potential of + 250 kV compared to the surface of the Earth. Ground based and satellite lightning observations (LIS and OTD), presented in Fig. 1, clearly show a marked contrast between lightning activity over land and ocean.

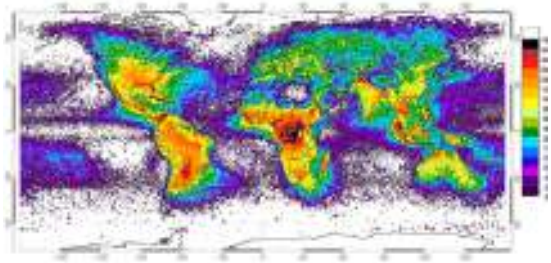

**Figure 1** – Global annual flash rate distribution obtained from the combined NASA LIS and OTD observations.

Two hypotheses have been formulated to explain the physical origin of this contrast. The thermal hypothesis is based upon the contrast between oceanic and continental surface temperatures. It simply considers that land lightning is dominant because land is hotter than ocean [1]. This hypothesis considers that the temperature correlated to the CAPE and consequently to the dynamical characteristics of thunderclouds, is a preferential parameter for the evaluation of the change in thundercloud electrification. The aerosol hypothesis [2] is based upon the aerosol concentration differences in the sub-cloud layer. Low aerosol and condensation nuclei concentrations, as in the case of oceanic thunderclouds, lead to premature formation of warm precipitation. Vertical velocities are thus inhibited, the concentrations of cloud drops and ice crystals (essential for the electrification process) in the mixed phase region are low and the optimal conditions for cloud electrification are reduced.

The purpose of this work is to determine if the thermal hypothesis alone may explain the cloud electrification process that leads to lightning production. In this paper, section 1 presents some elements of the classical thunderstorm climatology in Guadeloupe. In the following section, the cloud dynamical characteristics during days characterized by deep convective events are examined.

## Thunderstorm climatology in Guadeloupe

Data of thunderstorm occurrence reported by meteorological service (Météo-France Guadeloupe) have been collected for the 1973 - 2005 period. With 34 mean annual thunderstorm days, Guadeloupe is not one of the main tropical regions of occurrence of thunderstorm. Nevertheless, because of its geographical position which subjects it to an oceanic tropical climate, Guadeloupe becomes a place of interest to study the land-ocean contrast in lightning activity. Fig. 2 presents the annual thunderstorm day values and the yearly mean sunspot numbers [3] during the 1973-2005 period. One may note on one hand that for the first and the second cycle solar activity minima are back 2 or 3 years in comparison with thunderstorm activity minima. On the other hand, solar cycle peaks are relatively well correlated with the both first thunderstorm activity maxima. An inverse correlation between the decrease of solar activity in the last cycle and the two extreme values of thunderstorm activity in 2004 and 2005is also observed. However, the weak amount of data does not allow to make any conclusion in relation to the global change.

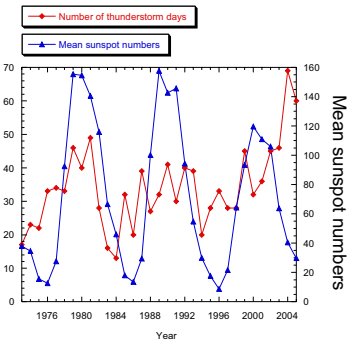


**Figure 2** – Annual thunderstorm days and yearly mean sunspots numbers for the 1973-2005 period.

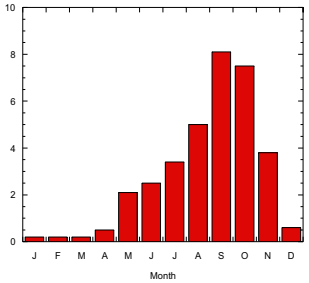


**Figure 3** – Monthly average number of thunderstorm days.

The climatological analysis is pursued by plotting the monthly average number of thunderstorm days (Fig. 3). It clearly situates the thunderstorm season in Guadeloupe from May to November with a peak of activity during September-October and a period of no (or very weak) activity from December to April. One note that transition from low activity to the activity peak spreads out on 5 months. The faster inverse transition only lasts 2 months. Then thunderstorm events during the 1973-2005 period have been separated by time of occurrence and their average durations have been calculated for each month.

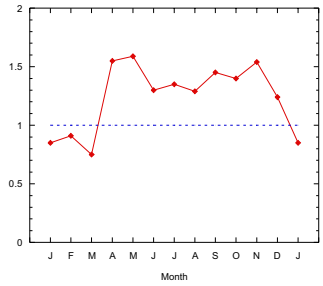


**Figure 4** – Monthly average duration of thunderstorm events (in hours).

Fig. 4 reveals that average duration of thunderstorm is larger than 1 hour from April to December and the greatest values (more than 1.5 hour) are observed for April, May and November. The hourly distribution of total number of events from 1973 to 2005 (Fig. 5) plainly presents a first peak between 12 AM and 03 PM (local time). This first peak, well correlated to the maximum value of temperature during the diurnal cycle, indicates that temperature is indirectly a control parameter for thunderstorm activity. In contrast, the results do not show the expected drop of thunderstorm activity between 03 AM and 05 AM. One may note the existence of a weaker secondary peak of thunderstorm activity. The latter is in inverse correlation with the temperature. Further, both peaks are present independently of the monthly electrical activity. As an example, Figure 6 presents the hourly number of thunderstorm events for the months of May and September, months that are respectively representative of low and high electrical activity.

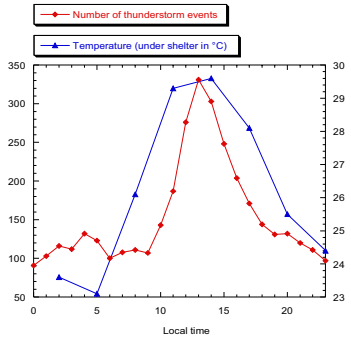


**Figure 5** – Hourly total number of thunderstorms events and mean diurnal variation of temperature during the 1973-2005 period.

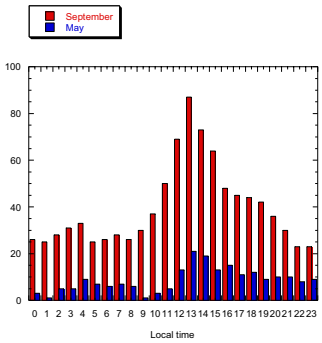


**Figure 6** – Hourly total number of thunderstorms events during the 1973-2005 period for May and September.

Finally, as may be seen in Table 1, thunderstorm days for a 4 year period (2002 - 2005) have been classified in 5 categories according to the type of weather. Roughly half of the thunderstorm events occur in synoptic conditions (for example, the passage of tropical disturbance, the proximity of the ITCZ during its yearly cycle). One can assume that under these conditions they are unlikely influenced by the thermal instabilities. Furthermore, if 28.8% of thunderstorm days from 2002 to 2005 were characterized by trade wind breakdown or weak trade winds, 37.1% of these days were thunderstorm days. During the trade wind breakdown or weak trade wind days one may suppose that both local thermal and aerosol concentration conditions influence thunderstorm activity.

**Table 1** – Percentage of thunderstorm days related to the type of weather from 2002 to 2005.

| | Thunderstorm days (%) |
|---|---|
| Sustained or strong trade winds | 0.0 |
| Undisturbed trade winds | 3.3 |
| Moist and unstable trade winds | 19.5 |
| Trade wind Breakdown or weak trade winds | 28.8 |
| Synoptic conditions | 48.4 |

## Cloud dynamical characteristics of deep convective events

Values of the following dynamical parameters: maximum cloud top height, maximum vertical velocity, CAPE and CIN have been computed for both thunderstorm days and days characterized by deep convection without production of atmospheric electricity. Computations were carried out for a 33 years period (1973-2005) using a 1D cloud model initialized with the corresponding appropriate atmospheric sounding. Then all cases with cloud top heights equal or higher than 7000 meters have been selected for this study. This choice is equivalent to the assumption that ice crystals, supercooled water and water vapour coexist above this altitude. Thunderclouds (hereafter referred to as TH clouds) are in average higher (roughly 7% as reported in Table 2) than clouds occurring during days characterized by deep convection (hereafter referred to as DC clouds). The same trend is observed in the case of maximum vertical velocity and CAPE values.

With an average value of 38 m/s, TH clouds seem develop larger maximum vertical velocities than DC clouds, and correspond to air masses characterized by roughly 19% to 24%

**Table 2** – Mean values of dynamical parameters for TH and DC days at 00 and 12UT

| | Maximum cloud top height (m) | | Maximum vertical velocity (m/s) | | CAPE (J/kg) | | CIN (J/kg) | |
|---|---|---|---|---|---|---|---|---|
| **Type of day and UT** | **Mean value** | **Standard deviation** | **Mean value** | **Standard deviation** | **Mean value** | **Standard deviation** | **Mean value** | **Standard deviation** |
| Thunderstorm days at 00UT | 12 709,4 | 1 147,1 | 38,1 | 11,5 | 1 903,3 | 539,3 | -468,3 | 301,3 |
| Thunderstorm days at 12UT | 12 621,5 | 1 291,6 | 38,4 | 12,2 | 1 926,1 | 595,5 | -482,9 | 353,8 |
| Days of deep convection at 00UT | 11 919,7 | 1 663,6 | 31,8 | 12,9 | 1 593,6 | 632,8 | -326,5 | 329,2 |
| Days of deep convection at 12UT | 11 730,3 | 1 722,8 | 31,8 | 12,7 | 1 559,3 | 632,0 | -320,2 | 338,7 |

larger values of CAPE. In contrast, mean CIN values are widely weaker in the case of TH clouds. Nevertheless, the high values of standard deviation for all theses parameters lead to examine first the distribution of the maximum cloud top height in relation to the corresponding cloud type (TH, DC). Figure 7 suggests that both TH and DC clouds preferentially have their tops in the 10000-15000 m range independently of the sounding hour.

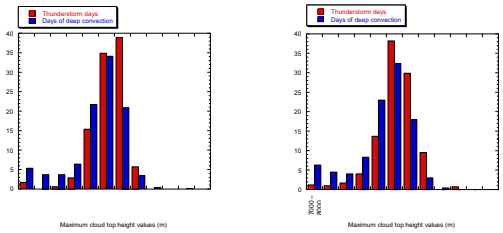


**Figure 7** – Percentage of thunderstorm days and days of deep convection in relation to maximum cloud top heights values (A – 00h UT soundings, B – 12h UT soundings).

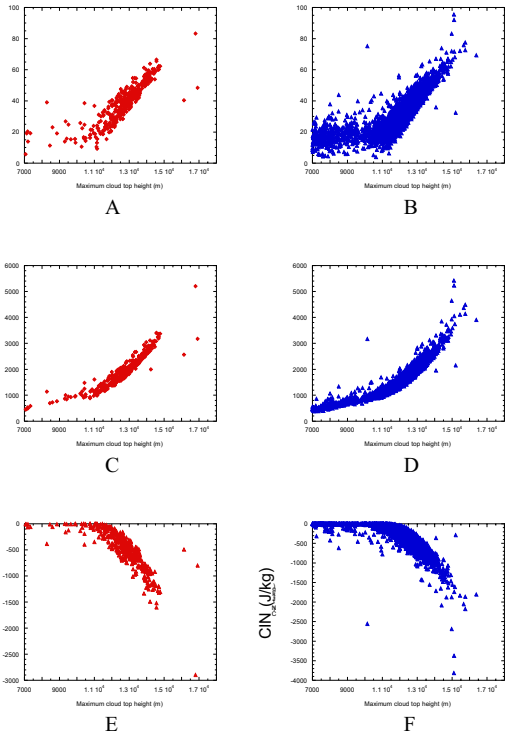


**Figure 8 –** Maximum vertical velocities (A, B), CAPE (C, D) and CIN (E, F) values in relation to maximum cloud top height values for 12UT soundings (A, C, and E – Thunderstorm days, B, D, and F – Days of deep convection).

Then, by representing maximum vertical velocity, CAPE and CIN values as a function of maximum cloud top height (Fig. 8), one can note that TH and DC clouds can clearly develop similar maximum vertical velocities, be characterized by similar CAPE and similar CIN in the 10000-15000 m range of maximum cloud top heights. The existence of deep convective clouds, with similar characteristics, that may or may not produce thunder, suggests that the dynamical indices studied in this work constitute deep convection indices and not cloud electrification indices. Obviously another parameter is most probably implicated in the cloud electrification process. This parameter could be the aerosol concentration in the subcloud layer.

## Conclusion

In a first time a climatological analysis of thunderstorm events has showed that during the diurnal cycle it appears a thunderstorm peak of activity from 12 AM to 03 PM in local time which is well correlated with the maximum values of temperature as supposed by the thermal hypothesis. Conversely, this hypothesis can not explain the presence of a weaker secondary peak from 03 AM to 05 AM.

Furthermore, by using a 1D cloud model, it have been shown that dynamical parameters such as maximum cloud top height, maximum vertical velocity, CAPE and CIN can not be used as indices for cloud electrification. They have to be most probably considered as convection indices that inform on deep convective cloud development.

Thermal and aerosol hypotheses should be envisaged as complementary. However further investigations on the influence of aerosol on thundercloud electrification are necessary.

## References

[1] E.Williams, S.Stanfill, The physical origin of the land-ocean contrast in lightning activity, C.R. Physique 3 (2002), 1277-1292.

[2] J.Molinié, C. Pontikis, A climatological study of tropical thunderstorm clouds and lightning frequencies on the French Guyana coast, Geophys. Res. Lett. 22 (1995) 1085-1088.

[3] ftp://ftp.ngdc.noaa.gov/STP/SOLAR_DATA/SUNSPOT_NUMBERS/

*Environment / Climate / Natural Hazards / Simulation*

# *Modelling of The Wind Field Produced During a Hurricane Passage In The Vicinity of An Island. A Case Study: The Island of Guadeloupe (FWI).*

*Kimathy ELISE*
*Université des Antilles et de la Guyane, faculté des sciences. LPAT-GEOL BP250*
*97157 Pointe-à-Pitre cedex, Guadeloupe - kimathy.elise@univ-ag.fr*

***Abstract***

The hurricane wind impact may have dramatic consequences on life, property and infrastructures if the hurricane trajectory crosses inhabited island regions. Thus, during the pre-crisis phase, simulation of the wind field in the layer close to the surface may constitute a powerful tool for deciders in the taking of decisions. In this paper, the preliminary investigations, drawn by means of simulation techniques in order to determine the wind field established by the interaction of a hurricane with an island's relief, are presented.

In this work, the Oklahoma University mesoscale model ARPS (Advanced Regional Prediction System) has been used in relation to the numerical terrain model of the island of Guadeloupe and cyclonic vortex bogusing techniques in order to infer the island boundary layer wind field as organized during the hurricane HUGO's passage (1989).

Two different numerical experiments have been drawn by using a large scale domain and a smaller one, corresponding to the same number of integration point domain but two different grid element lengths with lengths ratio equal to ten. The model initialization was made by means of the Météo-France local atmospheric sounding, whereby the hurricane was simulated by implementing an artificial (bogus) Rankine type vortex at a characteristic HUGO's centre trajectory location when the hurricane was close to the island, 16,18° latitude, -60,67° longitude at 9:30pm. Note that during these runs, the organization of the wind field resulted under the influence of the implemented island's relief and maximum sustained wind velocity as produced by the initial bogus.

Further, since the damage degree is proportional to the sustained wind velocity, a potential damage distribution may be extracted from the calculated wind fields and compared to the real damage.

Based upon the above mentioned conclusions, future investigations will concern the improvement of the bogus vortex in order to increase the accuracy of the real wind field conditions as well as the pertinent improvement of the relation between damages and sustained wind velocity in order to adapt this relation to the objective conditions of the island of Guadeloupe.

## 1. Introduction

Guadeloupe and many other islands in the Caribbean are more and more at risk of severe damage and life threatening conditions from wind danger produced by tropical cyclones since the number and strength of the hurricanes has increased due to the global warming.

These phenomena cause human losses and create enormous material damages thus costing a lot to the states. These are, among others, the reasons why means are set to work to understand intrinsically these atmospheric disturbances as to predict their trajectory and impact so that the current losses are reduced. For example, hurricane Ivan, in 2004, crossed Grenada at category 3 on the Saffir-Simpson hurricane Scale causing catastrophic damages, 85% of the island was ruined and 39 people was killed. Hurricane Hugo was the last destructive one that struck Guadeloupe Island in the night of September 16 to 17 1989. As a direct result of it 60% of the sugar cane plantation were destroyed, 466 millions of francs was needed to restore the banana fields, 35 000 persons became homeless and 7 persons were killed. It was a hurricane with sustained wind of 144 mph and strong gust from 163 to 187 mph. Hugo is serving as reference for a hurricane impact simulation in the presented work.

Hurricane modelling has already been studied to know its impact, Gary Y.K. Chocka and Leighton Cochran modelled the topographic wind speed effects in Hawaii and applied it to hurricane Iniki.

In this paper a study is carried out to see how the implementation of a wind field close to a hurricane can lead to the creation of vulnerability maps toward wind with the threatening of a hurricane coming through Guadeloupe.

The bogus vortex implemented for this use describes the radial profile of the wind and sets the pressure difference between the eye and the periphery, the radius of maximum wind is set plus the pulsation frequency. To study the wind field of the vortex over a numerical terrain of Guadeloupe, the Oklahoma University Mesoscale model ARPS (Advanced Regional Prediction System) is used.

A few words about the ARPS description will be given (the model capabilities), also, the hurricane Hugo characteristics will be depicted. Afterwards, the structure of the vortex and the simulation experiments will be explained and the results will be exposed and shown.

## 2. Description of the ARPS model

During the past few years, a model known as the Advanced Regional Prediction System (ARPS) has been developed at the Center for Analysis and Prediction of Storms (ARPS, Xue *et al.*, 1995) at the University of Oklahoma.The model is a non-hydrostatic, compressible atmospheric prediction model in a terrain following coordinate with equal spacing in *x* and *y* directions and the grid stretching in the vertical direction. It is used for scales ranging from a few meters to hundreds of kilometers. The model can be run in 1D, 2D and 3D modes. The ARPS model solves prognostic equations for *u*, *v*, *and w*, the *x*, *y*, and *z* components of velocity, the perturbation potential temperature $\theta$, and perturbation pressure *P*, sub-grid scale turbulent kinetic energy and the six categories of water variables such as water vapor, cloud water, rain water, cloud ice, snow and hail. Detailed description of the model, governing equations, the numerical methods, the physics parameterizations and computational implementation and configuration instruction are shown in the ARPS user's guide (Xue *et al* 1995).

### 3. Hurricane Hugo

According to Météo France information and data related by F.Pagney and E.Benito Espinal in "the hurricane Hugo", it arrived on the West-Indies with, in its centre, a minimum pressure of 942 hPa at the sea level, which is a low, but not extreme, value. In Raizet, Guadeloupe, it was 942hPA between & and 2am the 17 September. The anemometer was blocked shortly after the arrival but depicted maximum speed of 230 km/h (149 mph) at the eye approach and some wind gust from 26Okm/h to 300 km/h (162 to 186, 41 mph) affected the island. The active part of the hurricane spread over a 22Okm diameter, the spiral bands added 200km more of cloud clusters responsible of the persistent bad weather the whole day of 17 September The eye, that was really clear, seems to have had a diameter around 34 km. But this diameter was likely to have changed along the phenomenon way and the eye's shape seemed to be complex because it wasn't experienced the same way on the different locations where it passed. The radar of the meteorological service of Guadeloupe stopped to operate at 23 pm. The motion speed when it came to the eye island was 20 km/h (12,43 mph) which show some acceleration in some places, since on the sea, the speed was 19 km/h (11,81 mph). The first north wind started on the beginning of the evening and reached its peak from 11pm to 1:30 - 1:45am. The renewal of the strong wind where around 2:30-2:45 am, the wind was persistent until 4:30- 5am in the morning.

It is this persistence of violent wind that causes most of the damages, Hugo last ruthlessly a longer time than the previous hurricanes. The most ravaged disaster zone, in which the habitations were more damaged, follows a diagonal from St François, Ste Anne reaching to Petit Canal and Anse-Bertrand (Fig1). Désirade is included in this zone. This is also the area were the vegetation and the cultures were most affected.

*Figure1. Geographical distribution of the damages estimation*

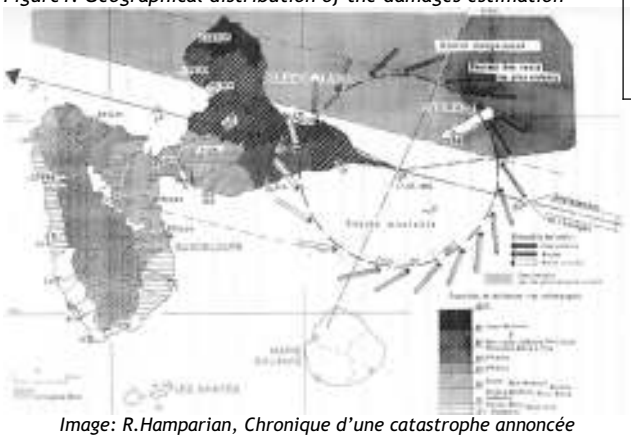

*Image: R.Hamparian, Chronique d'une catastrophe annoncée*

### 4. Simulation experiments

Tropical cyclones are one of the most difficult phenomena in the atmosphere to fully describe and predict even with access to highly sophisticated meso-scale models. Wind measurements from surface platforms, satellites, and aircraft reconnaissance may be available during and prior to landfall, but are seldom sufficient to describe the three-dimensional and constantly changing wind structures over the entire course of their existence. Engineers and scientists often resort to using parametric models to approximate the two-dimensional wind structure within a tropical cyclone in practical applications.

There are several parametric wind models, each of which has been shown to be valid and useful for at least one tropical cyclone event in a particular region. Essential to a parametric model is the representation of the wind flow in an idealized tropical cyclone by concentric circles. The wind speed is zero at the centre and increases rapidly to its maximum at the radius of maximum wind Rm and then decreases gradually to zero at large radii. This is the Rankine vortex in which the inner part turns as a disk and in the outer part the velocity is inversely proportional to the distance from the centre; i.e :

$v(r) = vm(r/ Rm)$ for $r \leq Rm$ (1)

$v(r) = vm/(r/ Rm)$ for $r \geq Rm$ (2)

where $v_m$ is the tangential velocity at r=Rm. In a cyclone "Rm" would be the radius of the eye wall.

Here a modified Rankine vortex is used. It has the particularity of traducing the inner organization of a hurricane; we can distinguish the eye, its wall and the external part considered as the spiral. Concerning the equations, it is different from the real rankine one by the fact that the wind speed is calculated with the expression (1) only for the disk representing the eye wall, the speed corresponding to the part of the ratio within the eye is zero.

*Tab1.Simulation initialisation*

| *Simulation* | EXP1 | EXP2 |
|---|---|---|
| Grid Centre | Lat: 16,18<br>Lon: -61,44 | Lat: 16,20<br>Lon: -61,44 |
| Resolution | 1km | 100m |
| Dimension | 660x660x35 | 660x660x35 |
| Modified Rankine Vortex | anr = 110.0,<br>omegacyc = 0.00825,<br>cyclat = 16.18,<br>cyclon = -60.67,<br>wvit = 1.0<br>u0 = -18.00<br>v0 = 6<br>autoconvnp = 0.0005<br>anre = 16.5<br>anrv = 56.0<br>dip = 70.0<br>ur = 0.5 | |

Anr: total hurricane ratio in *km*
Anre: eye ratio *in km*
Anrv: vortex ratio in km
Omegacyc: angular momentum
Cyclat: latitude of the vortex centre
Cyclon : longitude of the vortex centre
Wvit: vertical velocity inside the vortex
u0: translation speed E-W of the vortex *km/h*
v0: translation speed E-W of the vortex *km/h*! Autoconvnp: conversion rate of the cloud water in to rain water
dip: pressure difference between the centre and the periphery of the vortex
ur : radial velocity of the vortex

To know the impact of the wind of a hurricane it is important to study the phenomena at a good resolution to analyse the wind field over the Guadeloupe terrain. Thus, two different numerical experiments (Exp1, Exp2) have been drawn by using a 660x660x35 points integration domain. These experiments corresponded to two different grid element lengths of respectively **1**km and 100m). The model initialization was made by means of the Météo-France local atmospheric sounding, whereby the hurricane was simulated by implementing the modified Rankine type vortex at a characteristic Hugo's centre trajectory location when the hurricane

was close to the island, 16,18° latitude, -60,67° longitude at 9:30pm. At that time the wind speed was around 220km/h and progressively increase to 230km/h. The model results were taken after 1hour and 30 minutes of simulation at 11:00pm when the strong winds started in Pointe à Pitre.

The experiment Exp1 gives the wind parameter from the first coarse grid with 660km length and a 1km terrain resolution. These parameters are run in Exp2 in the fine grid with 66km length and 100m terrain resolution. Note that during these runs, the organization of the wind field resulted under the influence of the implemented island's relief and maximum sustained wind velocity as produced by the initial bogus vortex.

## 5. Results and Analyses

Results

*Figure2.1* *Exp1:*

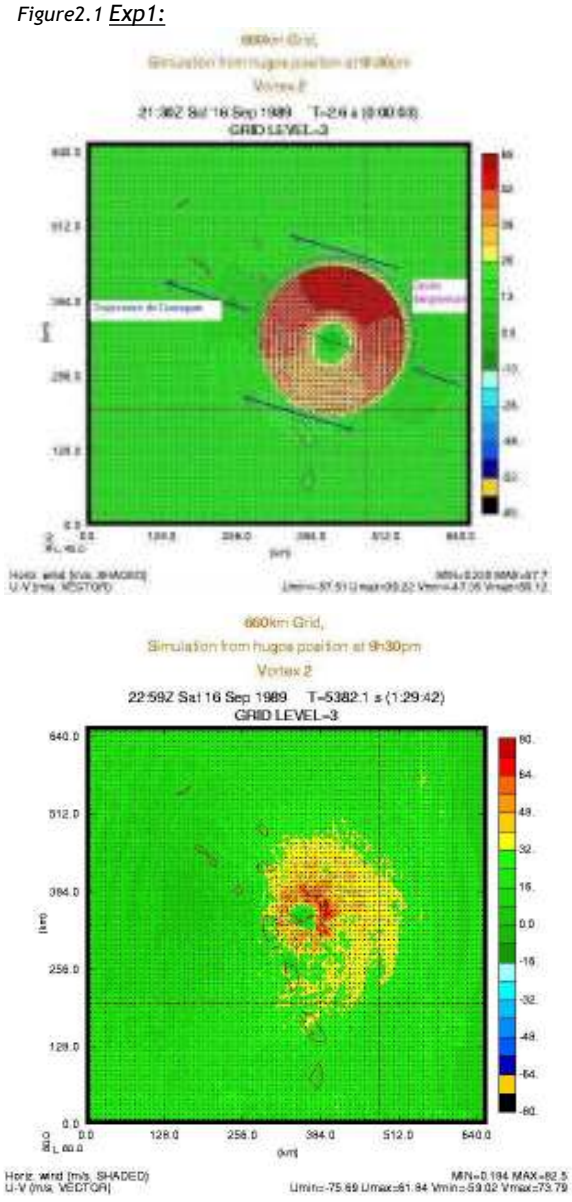


*Figure2.2* *Exp2:*

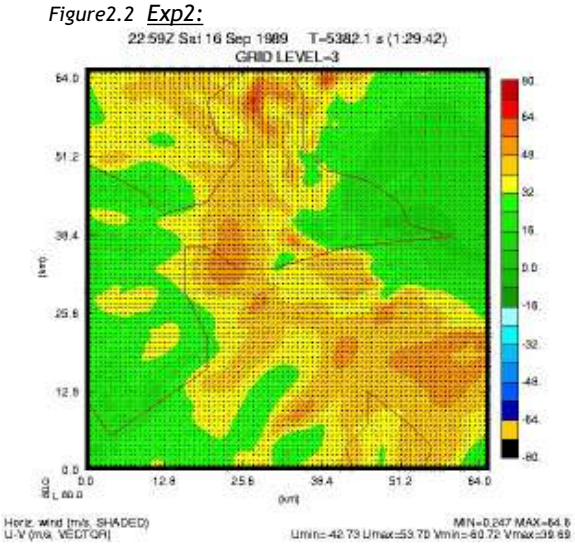


*Tab2.1. Table of u v w values of wind velocities in Anse-Bertrand (Massioux) zone*

| Latitude | longitude | u_component | v_component | w_component | qr | hterain |
|---|---|---|---|---|---|---|
| 16.403805 | -61.471703 | -0.924368 | -50.334469 | 4.264474 | 0.001036 | 9.826756 |
| 16.412863 | -61.471703 | -5.882792 | -52.663532 | 2.766037 | 0.001029 | 14.337385 |
| 16.421921 | -61.471703 | -6.073307 | -52.436192 | 1.908681 | 0.001346 | 19.423969 |
| 16.430979 | -61.471703 | -1.275618 | -51.857082 | 4.903445 | 0.001819 | 25.127672 |
| 16.440037 | -61.471703 | 1.029837 | -51.647030 | 9.215911 | 0.001791 | 31.453529 |
| 16.449095 | -61.471703 | -6.211184 | -49.968559 | 8.407942 | 0.001201 | 34.982761 |
| 16.458153 | -61.471703 | -20.913389 | -45.597721 | 1.105975 | 0.000975 | 37.342041 |
| 16.467211 | -61.471703 | -33.368221 | -42.061317 | -0.271710 | 0.001171 | 37.459557 |
| 16.476269 | -61.471703 | -34.549599 | -43.735725 | 5.700829 | 0.001145 | 32.764809 |
| 16.485327 | -61.471703 | -25.691101 | -47.825230 | 4.326044 | 0.001097 | 24.745712 |
| 16.494385 | -61.471703 | -19.126661 | -47.576447 | 1.188165 | 0.001201 | 17.465893 |
| 16.503443 | -61.471703 | -19.099751 | -42.433399 | 2.508601 | 0.001335 | 12.794712 |
| 16.512501 | -61.471703 | -20.084269 | -38.608051 | 3.614814 | 0.001460 | 8.855769 |
| 16.521559 | -61.471703 | -18.226631 | -38.815609 | 2.946603 | 0.001602 | 5.299107 |
| 16.530617 | -61.471703 | -13.918523 | -39.309109 | 2.599587 | 0.001834 | 2.215637 |
| 16.539675 | -61.471703 | -10.731243 | -37.957397 | 2.937972 | 0.002068 | 0.000000 |
| 16.548733 | -61.471703 | -11.612287 | -36.910351 | 3.505904 | 0.002268 | 0.000000 |

*Tab2.2 Table of u v w des values of wind velocities in Grands fond Ste Anne (Deshauteurs, St Protais zone).*

| Latitude | longitude | u_component | v_component | w_component | qr | hterain |
|---|---|---|---|---|---|---|
| 16.213587 | -61.426411 | 32.551445 | 3.324858 | -1.986142 | 0.001245 | 0.000000 |
| 16.222645 | -61.426411 | 31.313257 | -0.243378 | -2.795199 | 0.001149 | 6.851657 |
| 16.231703 | -61.426411 | 25.755281 | -7.816748 | -2.476076 | 0.001247 | 25.328421 |
| 16.240761 | -61.426411 | 26.607233 | -13.771370 | -2.316369 | 0.001403 | 51.459465 |
| 16.249819 | -61.426411 | 33.603600 | -17.870070 | -2.400411 | 0.001370 | 71.706734 |
| 16.258877 | -61.426411 | 34.111198 | -25.670208 | -3.074846 | 0.001018 | 88.296234 |
| 16.267935 | -61.426411 | 29.290289 | -34.735229 | -4.652631 | 0.000487 | 102.617226 |
| 16.276993 | -61.426411 | 17.729357 | -38.288403 | -3.721531 | 0.000262 | 107.079697 |
| 16.286051 | -61.426411 | 11.674391 | -34.552807 | -1.924759 | 0.000634 | 105.397766 |
| 16.295109 | -61.426411 | 21.527514 | -32.046589 | -1.805303 | 0.001152 | 97.128006 |
| 16.304167 | -61.426411 | 26.519556 | -33.860687 | -0.642535 | 0.001244 | 81.486313 |
| 16.313225 | -61.426411 | 19.041925 | -35.351566 | -0.238229 | 0.001061 | 58.956963 |
| 16.322283 | -61.426411 | 12.708139 | -35.234325 | 0.123919 | 0.001002 | 39.679840 |
| 16.331341 | -61.426411 | 14.834063 | -32.251419 | -0.658161 | 0.001085 | 26.183043 |

Analyses

The simulation shows that there's a clear distinction between the wind velocities in the "lethal part" of the hurricane and the other part. The wind values are more important in this side at the right of the hurricane trajectory. We can see that the areas of Guadeloupe that was under this part during the trajectory suffered more damages (fig 1, fig2.1, fig2.2, fig3).

The comparison of importance of the calculated wind velocities (Tab2.1, Tab2.2) and the percentage of damages occurred at different locations (fig3) suggests a close relation. Following the meridian -61,47° of longitude that is passing trough "Massioux" plateau in Anse-Bertrand that suffered heavy damages, we can notice too that model retranscribe the increase of the wind velocities from the sea zone in the north at latitude 16,54° where the wind speed is less important than in the higher elevation terrain at latitude 16,46°.

Same results are observed in "Les Grands Fonds" zone in Ste Anne.
Further, since the damage degree is roughly proportional to the third power of the sustained wind velocity, a potential damage distribution may be easily extracted from the calculated wind fields and compared to the real damage distribution as inferred from the insurance and state archives.

*Figure3. Damages Anse-Bertrand, Port-Louis, Petit-Canal*
% of damaged habitations by zones + comparison

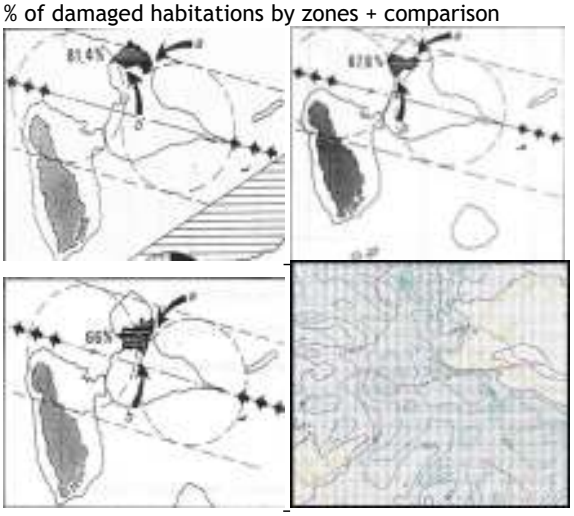

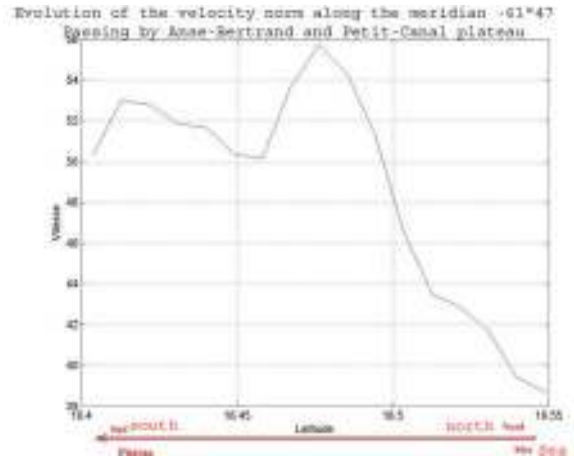


**6. Conclusion**

Based upon the above mentioned conclusions, future investigations will concern the improvement of the bogus vortex in order to increase the real wind field conditions as well as the pertinent improvement of the relation between damages and sustained wind velocity in order to adapt this relation to the objective conditions of the island of Guadeloupe. Thus, from modelling an up coming hurricane (the wind field and its trajectory), we can know the zone of the island that will be under danger. With a geographic study of the vulnerability factors and the vulnerable elements we can lastly make a vulnerability map towards a hurricane coming.

**References**

1. PAGNEY F. L'ouragan Hugo: genèse, incidences géographiques et écologiques sur la Guadeloupe, Ouvrage publié par le Parc National de la Guadeloupe, la DRAC de la Guadeloupe, le Parc Naturel Régional de la Martinique, 1992. L'Agence Guadeloupéenne de l'Environnement du Tourisme et des Loisirs, Fort-de-France. pp. 17-76.
2. Ming Xue, Kelvin K. Droegemeier, Vince Wong, Alan Sahpiro, Keith Brewster, (1995), ARPS Users's Guide, Center for Analysis and Prediction of Storms CAPS.
3. Gary Y.K. Chocka and Leighton Cochran. (2005) Modeling of topographic wind speed effects in Hawaii.
4. Robert Hamparian, Mémoire de Ter, (1994) université des Antilles et de la Guyane.
La Guadeloupe à l'épreuve de l'ouragan Hugo: *chronique d'une catastrophe annoncée*.
5. J. Thielen, A. Gadian
Influence of different wind directions in relation to topography on the outbreak of convection in Northern England, Ann. Geophysicae 14, 1078Ð1087 (1996) EGS Springer-Verlag 1996

*Environment / Climate / Natural Hazards / Simulation*

# Behavioral Change : An Original Application Of Health Belief Models For The Prevention Of Natural Hazards

NATHALIE MICHALON

*Département d'Anthropologie, Centre d'Etudes et de Recherche Caraïbes, Université des Antilles et de la Guyane - nathalie.michalon@univ-ag.fr*

**Abstract**

The Caribbean islands, located in a high potential seismic area with a great probability of volcanic eruptions, are moreover submitted to major meteorological phenomena. The prevention of these hazards, is vital for the entire populations of the Basin, where most of them use creole languages. The educational tools used in this domain must take into account the particular context in which each community lives, for a good understanding of the safety orders.

Lightning has shown to be harmful to both human and ecological life and can cause damage to the world's infrastructure. Through the lightning phenomenon narrative description, a practical and original method of behavioral change, using cognitive process based upon health belief models, is presented in this study.

## Introduction

The Caribbean islands, located in a high potential seismic area with a great probability of volcanic eruptions, are moreover submitted to major meteorological phenomena. The prevention of these hazards, is vital for the entire populations of the Basin.

Most of the people which are living in these countries are descendants of the African deportees by the Triangular Trade and which have developed their own culture by creolization process. Tales have an important place in these cultures because they allowed to transmit a part of the ancestral cultures.

Lightning has shown to be harmful to both human and ecological life and can cause damage to the world's infrastructure. Using a tale which describes the lightning phenomenon, we propose an original educational tool for the prevention of this hazard. Moreover, the social learning theory embedded in the story can be detailed for educational use in the case of behavioral change experiments.

Connections between weather and disease are well established, with many diseases occurring during certain seasons or erupting from flood or drought conditions. Climate change is likely to have various potential impacts on human health. In tropical countries, rising temperatures and humidity have facilitated the spread of many vector borne infectious diseases including malaria, dengue, Nile fever and recently chikungunya in Reunion island, because their transmission vector is the mosquito, which is sensitive to weather conditions (Tsai and Liu, 2005). Perceiving the susceptibility of the climate change problem, related to its impact on the human health, can be the starting point of a behavioral change in front of this situation.

## Materials & Methods

A narrative description of the lightning phenomenon, "From dust to lightning" (Michalon, 2005), had been elaborated in the form of a tale. During the travel inside a thundercloud, the readers are driven from a bubble in the ocean until the production of a lightning. For a best understanding for the creole speaking people from Haïti, Saint-Lucia, Dominica, Guadeloupe, Martinique and French Guyana, it was been translated in kréyòl, entitled "Kont a van é gout". Physics contained in the text are exact (McGorman and Rust, 1998; Pruppacher and Klett, 1978).

The 5 chapters present the following descriptions:

Chapter 1: the bubble burst mechanism

Chapter 2: the coagulation process and turbulent movements in the atmosphere

Chapter 3: the greenhouse effect and the buoyancy
Chapter 4: the rainfall formation process
Chapter 5: the freezing and crystallization process ; the sparks and lightning production.
Embedded in the story, a social learning theory which takes into account cognitive process, allow to memorize the stages of belief model used in behavioral change experiments.

**Structure and cognitive process**

The pivotal notion of "structure" is defined as a system of transformations which abides by certain laws and which sustains or enriches itself by a play of these transformations, which occur without the use of external factors (Piaget,1978). This auto-structuration of a complete whole is defined as "auto-regulation". In the individual, the latter is established by biological rhythms, biological and mental regulations and mental operations. These can be theoretically formalized.
The existence of all living substances begin with action and this is rooted in biological processes. Action implies the formation of cognitive structures which are at first exteriorized in coordinated external movements. After repeated actions, interiorization, permanency, invariant principles and imagination allow for the emergence of internal cognitive structures. So the following sequence appears :

1 external actions (system) and reactions (environment) ;
2 . interiorization and permanency ;
3 internal cognitive structures and auto-regulation ;
4 novel external actions.

These internal cognitive structures are constantly being transformed and regulated in order to adapt the system to new situations. This process is recurrent and so always more complex cognitive structure emerge.

**Health Belief Model and behavioral change**

A Health Belief Model, developed in the 1990s by Prochaska and colleagues, holds that health behavior is a function of individual's socio-demographic characteristics, knowledge and attitudes (King, 1999). According to this model, individuals or groups pass through 6 stages in order to be able to change behavior. They are:
1) pre-contemplation (Perceiving susceptibility to a particular problem)
2) contemplation (Perceiving seriousness of the condition)
3) preparation (Belief in effectiveness of the new behavior)
4) action
5) maintenance (Perceiving benefits of preventive action)
6) relapse (Perceiving barriers to taking action)
In this model, promoting action to change behavior includes changing individual personal beliefs.
Individuals weigh the benefits against the perceived costs and barriers to change.

**Results & Discussion**

Historically, the tales were socially and psychologically best suited to the condition of the people in the Caribbean islands during the slavery period because they allowed them to express their fantasies and their deepest anxieties (Tiffin, 1982). Creolization is defined as " a cultural action, material, psychological and spiritual based upon the stimulus response of individuals to their environment" (Brathwaite, 1971). In that way, tales can act as creolization responses to a new environment, dramatizing efforts to manipulate it verbally and symbolically and they can become measures of self-reliance and self-affirmation (Tortello, 1991).
The continuous emancipation of the different cognitive forms of equilibrium (an always increasing cognition) is a pivotal notion in the behavioral change process. This increase is the natural result of successful re-equilibrations, in which logico-symbolical functions plays a major role. Auto-regulation is also the result of the interactions between the system and its environment. Hence, intersubjectivity is always essential in the construction of new and stronger cognitive structures. This implies that cognitive processes not only appear as resulting from organical auto-regulation of which they reflect

the essential mechanisms, but also emerge as differentiated organs of this regulation in the arena of interactions with the environment. Cognition is the most differentiated biological organ of survival human beings have. Social cognitive or social learning theory states that new behaviors are learned either by modeling the behavior of others or by direct experience. It focuses on the important roles played by vicarious, symbolic, and self-regulatory processes in psychological functioning and looks at human behavior as a continuous interaction between cognitive, behavioral and environmental determinants (Bandura, 1977). In order for an intervention to be successful, the model must target the appropriate stage of the individual or group which pass through all stages, but do not necessarily move in a linear fashion (Prochaska, 1994). The stages of change model emphasizes the importance of cognitive processes and movement between stages depends on cognitive-behavioral processes.

Consequently, the tale "From dust to lightning", which includes recent social learning theory for behavioral change, can be used for the prevention of natural hazards, particularly for the electrical risks related to lightning struck and for the climate change prevention, and as well in several domains which need educational tools for behavioral change (health problem and HIV/AIDS prevention, industrial risks prevention, etc.). Moreover, in the Caribbean islands, the illiteracy is a major problem for the prevention programs. Translations in creole languages would allow to transmit safety orders with a better understanding from creole speaking people.

## References

1. Bandura A., (1977). Social learning theory. Prentice-Hall, Inc., Englewood Cliffs, New Jersey 07632.

2. Brathwaite, E. K. (1971). The Development of Creole society in Jamaica. Oxford: Clarendon Press.

3. King R. (1999). Sexual behavioural change for HIV: where have theories taken us?, Joint United Nations Program on HIV/AIDS, UNAIDS Best Practice Collection.

4. MacGorman, D.R., and W.D. Rust (1998). The Electrical Nature of Storms, Oxford University Press.

5. Michalon N. (2005). From dust to lightning, Paljor Publications Ltd.

6. Piaget J. (1978). Le structuralisme, Que sais-je ?, éditions PUF, 12ème édition (1996).

7. Prochaska J., Redding C., Harlow L., Rossi J., Velicer W. (1994). The transtheoretical model of change an HIV prevention: a review, Health Ed Quartely 21 (4) , 471-486.

8. Pruppacher H.D. and J.D. Klett (1978). Microphysics of cloud and precipitation, D. Reidel Edition , Higham, USA.

9. Tiffin, H. (1982). "The metaphor of Anancy in Caribbean literature" in Sellick, R. (Ed). Myth and metaphor.
Adelaide: Centre for Research in New Literatures in England

10. Tortello, R. (1991). "The Magical spider-man: The Metaphormoses of Bredda Anansi." Diss. Harvard University.

11. Tsai H.T., Liu T.M. (2005). Effects of global climate change on disease epidemics and social instability around the world, Human Security and Climate Change, International Workshop, Asker (Oslo), 21-23 June.

*Environment / Climate / Natural Hazards / Simulation*

# Two Numerical Experiments For The Investigation Of Possible Influences Of A Climate Change On The Global Atmospheric Electrical Circuit

NATHALIE MICHALON

*Agence KaNNH, Saint-Joseph, Martinique - nathalie_michalon@yahoo.fr*

**Abstract**

Evidence is emerging for physical links among clouds, global temperatures, the global atmospheric electrical circuit and cosmic ionization. Atmospheric electrical modification of cloud properties may have significant global implications for climate, via changes in the atmospheric energy balance. Likewise, global temperature changes have been suggested as a source of variability in the global atmospheric electrical circuit.

In this study, in order to infer the impact of a global climate change on the atmospheric electrical circuit, two numerical climate change experiments with respectively doubled CO2 concentration and a 3% continental cloud cover decrease have been made.

Both numerical experiments lead to a roughly 10% increase of the mean global annual flash frequency, that corresponds to a mean global surface warming of 1.92 K.

## Introduction

The lightning production of thunderstorm clouds is of interest in different fields of research, engineering and civil protection. It is usually expressed in terms of lightning frequency F which is a function of the thunderstorm cloud electrification degree and is related to the dynamical and microphysical cloud characteristics (Price and Rind, 1992; Rutledge et al., 1992; Molinié and Pontikis, 1995; 1996; Michalon et al., 1999). It has been suggested that lightning activity might be used as a sensitive indicator of changes in climate (Williams, 1992; 1994; Reeve and Toumi, 1999).

Moreover, recent observations indicate electromagnetic waves association with earthquake. The emission of these waves as a result of electric charge redistribution is one of the main hypothesis regarding the waves generation mechanism (Singh et al., 2002).

In this study, in order to infer the impact of a global climate change on the atmospheric electrical circuit, two numerical climate change experiments with respectively doubled CO2 concentration and a 3% continental cloud cover decrease have been made.

## Materials & Methods

The Michalon et al. (1999) flash frequency parameterization has been obtained by combining the

Price and Rind (1992) analysis results, the Molinié and Pontikis (1995) conclusions suggesting that the cloud droplet concentration is a key parameter for cloud electrification, and simple dimensional arguments. It may be written as

$$F = 4.392 \times 10^{-7} N^{2/3} H^{4.9}$$

where H is the cloud height and N the cloud droplet concentration.

In the numerical experiments, we use two "standard" droplet concentration values (Nc = 600 cm-3 and Nm = 50 cm-3) respectively valid for continental and maritime clouds.

The determination of the relative proportion of cloud-to-ground flashes uses the empirically derived formulation (Price and Rind, 1994):

$$P = 1/ (aD^4 + bD^3 + cD^2 + dD + e)$$

where a, b, c, d and e are the appropriate coefficients, and D the cold cloud thickness.

An analysis by Marsh and Svensmark (2000), shows that cosmic rays and low (i.e. with altitudes less than about 3 km) clouds observed by global satellites are strongly correlated around the cosmic ray minimum of 1990. The correlation was originally presented in 1997 (Svensmark and Friis-Christensen, 1997) and the

limitations of the data analysis and acquisition have been the subject of considerable discussion (Kernthaler et al., 1999; Kristjánsson and Kristiansen, 2000). There is no correlation with high clouds (Kristjánsson and Kristiansen, 2000). However, variations in the ionospheric potential has been linked to cosmic ray variations arising from the solar cycle (Markson, 1981).

The "ARPEGE-IFS-cycle 14" GCM used for the numerical experiments has been developed jointly by Meteo- France and the European Center for Medium Range Weather Forecasts (ECMWF) and has been adapted by Déqué et al. (1994) for climate purposes. The model has been validated at various horizontal resolutions in 10-year integrations using prescribed monthly mean sea-surface temperatures observed between 1979 and 1988 (Déqué et al., 1994). The cloud top heights used to infer the flash frequencies are obtained from two different numerical experiments hereafter referred to as 1×CO2 (control simulation) and 2×CO2 (global warming simulation) concerning the time period between the 28 October 1998 (0.00 UT) and 27 October 1998 (24.00 UT). As the model is purely atmospheric, the sea surface temperatures (SSTs) are prescribed as external boundary conditions, whereby the methodology known as "time-slice simulations" (Mahfouf et al., 1994; Timbal et al., 1997) is used. In 2×CO2 experiment, the ocean response to increased greenhouse warming is taken into account by adding to the climatological SSTs of 1×CO2 experiment, the ocean warming simulated at the time of CO2 doubling in a fully coupled transient scenario performed with the Hamburg ocean-atmosphere coupled model (Cubasch et al., 1992).

In order to infer the influence of the solar cycle on the climate, the second experiment is a rough test of the impact of a 3% continental cloud convective cover decrease on the global electrical circuit, whatever the cause of the cloud cover change.

**Results & Discussion**

The global circuit consists of the ionosphere, Earth's surface, fair-weather current and thunderstorm current. Within the ionosphere, the positive charge is carried to areas of fair weather, and small currents flows vertically. In order for the spherical capacitor to remain charged, there must be a mechanism that acts to re-supply the charge to close the electrical circuit. Thunderstorms are the most common forms of disturbed weather that cause local electric fields to be produced and cause positive charge to move upwards toward the ionosphere and negative charge to move to the surface (Wilson, 1920).

The fair-weather current is the flow of current from the positively charged ionosphere to the negatively charged Earth's surface in regions of fair-weather. The vertical atmospheric electric field E(z) is derived from the measured potential V at a height z. The ionospheric potential VI which is obtained from vertical sounding of the variation of E(z) with height, is the potential of the lowest conducting regions of the ionosphere, reckoned with respect to a zero potential at the surface.

The control simulation (1×CO2) results are in good agreement with the recent observations of the lightning frequency distributions (Christian et al., 2003). The variation of the global diurnal lightning cycle obtained from the numerical control experiment are in good agreement with the variation of the measured fair-weather potential.

The 2×CO2 experiment shows a 9.8% increase of the mean global flash frequency which corresponds to a mean global surface warming of 1.92 K. The experiment of a decrease of the convective cloud cover shows a 12.9 % increase of the global flash frequency. Both experiments show similar variations of the flash frequency distribution.

Changes in thunderstorms caused by surface temperature changes would cause modulations on the global atmospheric electrical circuit. Increases in surface temperature leading to more vigorous convection have been quantitatively linked with increases in VI (Price, 1993), offering a possible indirect method of monitoring surface temperatures. A positive correlation between global temperature datasets and VI was observed, supporting a relationship

between warmer temperatures and an increased VI (Markson and Price, 1999). A global increase of the ionospheric potential VI linked with increases in global surface temperature would change the charging of the global electric circuit. A small observed modulation in VI has been linked to cosmic ray variations arising from the solar cycle (Markson, 1981) : cosmic ray ionization modifies the atmosphere's columnar resistance. VI increased when an increase in cosmic rays occurred. Markson (1981) showed that, for the increase in cosmic rays to increase VI , the change has to influence the charging part of the global electrical circuit.

Although the effects of electric fields on cloud physical processes are not well understood, an increase of the cloud electrification would result from an amplified fair-weather current or an enhanced conductivity in the lower stratosphere (Markson and Muir, 1980). Flash frequency lightning distributions and particularly the diurnal lightning cycle which follows the fair-weather current variation, would be interesting parameters to estimate the earth's electric field evolution, linked or not to a global warming.

**Acknowledgements**

The results of climate modeling used in this study are issued from the work made in the Laboratoire de Physique de l'Atmosphère Tropicale, Université des Antilles et de la Guyane, in the frame of my PhD thesis. I thank all the LPAT's members for their support and their hospitality.

**References**

Christian H.G. et al. (2003). Global frequency and distribution of lightning as observed from space by the Optical Transient Detector, J. Geophys. Res., 108(D1), 4005, doi:10.1029/2002JD002347.

Cubash U., Hasselman K., Höck H., Maier-Reimer E., Mikolajewicz U., Santer B.D., Sausen R. (1992). Timedependent greenhouse warming computations with a coupled atmosphere-ocean model, Climate Dyn., 8, 55-69.

Kernthaler S.C., Toumi R. and Haigh J.D. (1999). Some doubts concerning a link between cosmic ray fluxes and global cloudiness, Geophys. Res. Lett., 26, 7, 863-865.

Kristjánsson J.E. and Kristiansen J. (2000). Is there a cosmic ray signal in recent variations in global cloud cover and cloud radiative forcing? J. Geophys. Res., 105, 11851-11863.

Mahfouf J.F., Cariolle D., Royer J.F., Geleyn J.F., Timbal B. (1994). Response of the Météo-France climate model to changes in CO2 and sea surface temperature, Climate Dyn., 9, 345-362.

Markson R. and Muir M. , 1980 : Solar wind control of the Earth's electric field, Science, 208 (4447), 979-990.

Markson R. (1981). Modulation of the earth's electric field by cosmic radiation, Nature, 291, 304-308.

Markson R. and Price C. (1999) Ionospheric potential as a proxy index for global temperature, Atmos. Res., 51, 315-321.

Marsh N. and Svensmark H. (2000). Low Cloud Properties influenced by Cosmic Rays, Phys. Rev. Lett., 85, 23, 5004-5007.

Michalon N., Nassif, A., Saouri, T., Royer, J. F., Pontikis C., 1999: Contribution to the climatological study of lightning ,Geophys. Res. Let., 26(20), 3097-3100.

Molinié J. and Pontikis C.A. (1995). A climatological study of tropical thunderstorm clouds and lightning frequencies on the French Guyana coast, Geophys. Res. Lett., 22(9), 1085-1088.

Molinié J. and Pontikis C.A. (1996) Reply, Geophys. Res. Lett., 23(13), 1703-1704.

Price C. (1993). Global surface temperatures and the atmospheric electrical circuit, Geophys. Res. Lett., 20 (13), 1363-1366.

Price C., Rind D. (1992). A simple lightning parameterization for calculating global lightning distributions, J. Geophys. Res., 97, 9919-9933.

Price C., Rind D. (1994). Modeling global lightning distributions in a general distribution model, Mon. Wea. Rev., 122, 1930-1939.

Reeve N. and Toumi R. (1999).Lightning activity as an indicator of climate change, Q. J. R. Meteor. Soc., 125, 893-903.

Rutledge, S.A., Williams E.R., and Kennan T.D. (1992). The down under Doppler and electricity experiment (DUNDEE): Overview and preliminary results. Bull. Amer. Meteor. Soc., 73, 3-16.

Singh R.P., Patel R.P., Ashok K Singh (2002). Lightning generated ELF, VLF, optical waves and their diagnostic features, Indian J. Phys., 76B (3), 235-249.

Svensmark H. and Friis-Christensen E. (1997). Variations of cosmic ray flux and global cloud coverage - a missing link in solar-climate relationships, J. Atmos Sol.-Terr. Phys., 59, 1225 - 1232.

Williams E.R. (1992) The Schumann Resonance: a global thermometer. Science, 256, 1184-1187.

Williams E.R. (1994) Global circuit response to seasonal variations in a global surface air temperature. Mon. Wea. Rev., 122 , 1917-1929.

Wilson C.T.R. (1920). Investigations on lightning discharges and on the electric field of thunderstorms, Phil. Trans. Roy. Soc. Lond., A221, 73-115.

*Environment / Climate / Natural Hazard / Simulation*

**Facing Natural Hazards: Policies, Strategies, role of Basic Sciences**

LILLIAM ALVAREZ DIAZ,

*Director of Sciences, Ministery of Science, Technology and Environment of Cuba - lilliam@citma.cu*

**Abstract**

The lecture will include some historical review of natural hazards in the island, comments and reflections of the social and governmental organization, civil defence, political strategies and policy of science and technology for facing mainly, tropical hurricanes.

Effective R&D systems to mobilize science and technology for sustainable development is not an impossible to design and implement, if the countries start for *a political will* to face, in first place the natural hazards. The Cuban experience has proved this.

Cuba has made many in implementing integrated Strategies and System of S&T and Environment, problem-driven, capacity building, place-based research and applications Programs in support of sustainability.

Some practical experiences, data, figures, indicators will be posed in the lecture and also methodologies and practical measures to minimize the impact of tropical organisms in general.

The importance of having human resources well prepared, educated, and a "critical mass" of scientists, engineers, modest infrastructures in R&D centers, programs and projects, including capacities in basic sciences, as Physics, Mathematics and Computational sciences, besides, good meteorologists, will be discussed.

The role of the media, the effective, real and veridical information by radio, newspapers, e-mails, internet, TV and different ways of preparation and social communication of the measures previous, during and after the disaster also will be a topic for the debate.

**CDSA: A New Seismological Data Center for French Lesser Antilles**

M. BENGOUBOU-VALÉRIUS (1), D. BERTIL (2), S. BAZIN (3), A. BOSSON (4), F. BEAUDUCEL (4) and A. RANDRIANASOLO (1)

*(1)EA921 LPAT-GEOL, Université Antilles-Guyane, Guadeloupe - bengoubou@yahoo.fr*

*(2) Service géologique régional, BRGM, Guadeloupe*

*(3)OVSM, IPGP, Martinique - (4)OVSG, IPGP, Guadeloupe*

**Abstract**

The Lesser Antilles is an area of high volcanic and earthquake activity, characterized by a 1000 km convergence zone resulting from the Atlantic plate subduction under the Caribbean plate with a slow convergent motion (2 cm/year). This arc has a specific regional setting with important structural heterogeneities which can affect seismic characteristics: oblique subduction in the North, large accretion prism in the South, aseismic ridge sinking in subduction, shallow intraplate active faults close to the volcanic arc. In 2000, the "*Centre des Données Sismologiques des Antilles*" (CDSA) was created, with the purpose to provide seismological data at public disposal for multiple applications: research, earthquake engineering, and pedagogic. To reach this objective, it is necessary to gather all Martinique and Guadeloupe seismological data, presently scattered between several institutions and in different numerical formats; then, to process data to make them compatible and produce more accurate information on regional and local seismic activity. Numerical signal records and phases arrival times bulletins come mainly from permanent volcanic and seismologic survey networks managed by IPGP Observatories and several accelerometric networks. More than 120 stations from 10 networks with short period, broadband or accelerometric sensors are concerned. With five years of available data, the

CDSA data base presents a more homogeneous vision of Lesser Antilles arc seismicity and allows detecting low seismic activity zones, in the north near the Virgin Islands, and in the south between St-Lucia and Grenada. The accuracy improvements of CDSA location, evidenced by the study case of Les Saintes 2004 swarm, is used to better study the relationship between tectonic structures and seismicity around Guadeloupe and Martinique islands, and to better define the subduction slab geometry. Cross-sections perpendicular to the arc reveal that the slab has a nearly constant, 50° dip angle, from St-Lucia to Nevis. As seismic hazard assessment depends from strong ground motion generated by earthquakes, the CDSA data base also includes strong motion records of the region. The underestimation of the peak acceleration values by standard attenuation laws at large distances shows the need to develop new formulae adapted to the Lesser Antilles context.

**References**: F.W.Klein, 2002, U.S.G.S. Openfile report 02-171.

## Seismogenic Potential of Fore-Arc Tectonic Structures: Onshore - Offshore Geology Helps to Understand the Tectonic Activity at the Marie-Galante Basin - Lesser Antilles

J.F. LEBRUN (1), J.L. LÉTICÉE (1), S. BES DE BERC (2), J.J. CORNÉE (3), P. MUNCH (4), A. RANDRIANASOLO (1), I. THINON and M. VILLENEUVE (1)

*(1) EA 923 LPAT-GEOL, Université des Antilles et de la Guyane, Pointe à Pitre, FWI - jflebrun@univ-ag.fr*
*(2) BRGM, Le Houëlmont, Gourbeyre, FWI*
*(3) UMR 5125 PEPS, Université de C. Bernard - Lyon 1, Villeurbanne, France*
*(4) FRE 2167 GSC, Université de Provence - Marseille, France*

**Abstract**

Estimating seismogenic potential of active faults is a challenge that requires short and long term evaluation of faults activity. Therefore, the planform of fault systems as well as average velocity of deformation over periods ranging from 102, 106-7 years are key parameters to estimate magnitude and return period of earthquakes.

The Marie-Galante basin is a tectonic graben transverse to the lesser-Antilles fore-arc that accommodates the N-S extension of the fore-arc in response to oblique subduction. The graben abuts the Soufrière Volcano (Guadeloupe) to the west, and it is bounded along both sides by normal faults with clear morphological expression. These faults were identified onshore and offshore. Recent estimates of vertical displacement along one onshore segments of a fault at the southern border of the basin provides slip rates of $0.5 \pm 0.2$ cm/year over the last ca. 330Ma. A rough estimation of the maximum earthquake magnitude the fault can generate gives $M = 6.5$ with a recurrence time of 1400-3300 years (Feuillet et al, 2004). More precise estimates of earthquakes hazard require to investigate the exact 3D geometry of fault systems in the graben, and to quantify the evolution and propagation of the faults through time.

We newly interpreted seismic reflection profiles in the offshore basin to constrain the geometry, the timing and the evolution of the fault systems in the graben. This study permits to sort out the active faults and to identify several incipient structures. We also identified inactive faults systems and established a relative chronology of the fault propagation. We highlight the total amount of displacement accommodated along the various faults. Onshore our description of the stratigraphic records of the carbonate platform in Marie-Galante and Grande Terre (Guadeloupe) in terms of paleo-environment and paleo-bathymetry reveals the influence the glacio-eustatic variations versus the tectonic contribution. Our study helps to constrain the age of the tectonic inception in the Marie-Galante Basin. Offshore sampling of geological series, due in late 2006 and 2007, will allow us to date the tectonic activity along the faults and, eventually, will lead to a quantification of the deformation and a more precise estimation of earthquakes hazard.

*Environment / Climate / Natural Hazard / Simulation*

**Evaluation of the Tsunami Risk for Guadeloupe (Lesser Antilles)**

N. ZAHIBO (1), E. PELINOVSKY (2) and I. NIKOLKINA (3)

*(1) Laboratoire de Physique Atmosphérique et Tropicale, Département de Physique, Université Antilles Guyane, Pointe-a-Pitre, France - narcisse.zahibo@univ-ag.fr*
*(2) Laboratory of Hydrophysics, Institute of Applied Physics, Nizhny Novgorod, Russia Pelinovsky@hydro.appl.sci-nnov.ru*
*(3) Department of Applied Mathematics, Nizhny Novgorod State Technical University, Nizhny Novgorod, Russia - inikolkina@mail.ru*

**Abstract**

Available data of tsunami manifestation in Guadeloupe (Lesser Antilles) for 500 years is analysed and discussed. Highest values of the tsunami heights have been recorded in the northern Guadeloupe (Basse-Terra Island). Numerical simulation of the wave height distribution along the coast of Guadeloupe is performed in the framework of shallow water theory for several possible locations of the tsunami sources, and also for historic 1867 and 2003 events. Results of the numerical simulations confirm that tsunami waves approached to Guadeloupe have large values in its northern part.

**North Atlantic Hurricanes Trajectories; Important Forecast Parameters: a Case Study, 2006 Hurricane Season**

G. LEQUELLEC, C. ASSELIN DE BEAUVILLE

*Laboratoire L.PA.T/G.EO.L, Université des Antilles et de la Guyane, 97159 Pointe à Pitre Guadeloupe - christian.asselin@univ-ag.fr*

**Abstract**

The poster presented is based on reseach from data of LPAT laboratory collected from 1996 to now. These data include photographies of GOES 12 satellite and A.V.N. model output. A.V.N models maps starts only in 2000. First we define the characteristic of hurricane track in Atlantic Ocean. All the tracks can be represented by three mean groups that is to say, extreme North paths in atlantic ocean, mid North which can reach the U.S coasts and South which can go accross the Lesser antilles Archipelago.

Next we study the influence of lower and higher pressures centers. The major influence of low-pressure center is to attract, while high-pressure systems makes curvatures. Recent cases are showed. Localisation of high-pressure centers are a crucial factor. Their evolution can be linked to N.A.O ( North Atlantic Oscillations) as S.O.I. (South Oscillations Index) in Pacific Ocean. N.A.O index is necessary to determine the intensity of winter in Europe. This index associated with S.O.I. index may be useful to try to forecast the crossing of Lesser Antilles Archipelago; if not, the tracks recurve to the North. A data table for the past twenty years is showed. El nino phenomena as a inhibitive role. When la Nina phenomena is present and NA.O. index is negative, this is factor of risk for our Archipelago.
At last we show the predictors for 2006 season. The lack of El Nino can contribute to the crossing of a intense hurricane through or near the Lesser Antilles Archipelago.

*Environment / Climate / Natural Hazard / Simulation*

# A Method of Analysis and Identification of Clouds of Satellite Images Coming from GOES Satellite

J. NAGAU AND J-L HENRY

*Laboratoire GRIMAAG , Université des Antilles et de la Guyane, Département Mathématiques et Informatique, B.P. 592, 97159 Pointe-à-Pitre Cedex - jnagau@univ-ag.fr, jlhenry@univ-ag.fr*

**Keywords**
Image analysis, pattern recognition, classifier systems, classification, supervised training, database knowledge.

**Abstract**

The purpose of our work is to provide physicists and meteorologists with an application capable of determining from satellite pictures taken in the field of visible and infrared lights the types and percentages of clouds present [1] to establish a climatic cartography of the Caribbean area. We take into account three types of clouds : the cirrus situated in the superior layer in approximately six kilometers in height, the cumulus in the lower layer than five hundred kilometers in height and the stratus which can be observed in the intermediate layer in two kilometers in heights. Our method consists by extracting discriminating characteristics of the various types of cloud heaps discovered on the images to make a classification. We carry out a sequence of operations appropriate for the theory of shape recognition [2] which, at first enables to track down the pixels which belong to clouds [3] and then, to extract information from the aggregates of points found. The image taken in the field of visible light enables to know if we are dealing with thick clouds or about thin cloud layers. Indeed, the thin layers of clouds are not detectable in the image taken in the visible light whereas the thick clouds appear clearly. This phenomenon is due to the fact that the very thin layers do not reflect the light. The elements we exploit are : the shapes of the cloudy heaps, the variations of pixels belonging to clouds, the clouds brightness. These values are coded in binary and concatenated with a view to achieving an interpretation from LCS (Learning Classifier Systems) type systems [4]. Every cloud is represented by a binary chain will be associated with one of the three classes. Before becoming autonomous, the system will need a supervised training period to set up its base of knowledge and correct the classification errors [5].

**References**

[1] Weather satellites: systems, data, and environmental applications, P. Krishna Rao, Susan J. Holmes, Ralph K. Anderson, Jay S. Winston, and Paul E. Lehr, American meteorological society.
[2] Reconnaissance des formes, Méthodes et applications, Abdel et Yolande Belaïd, Inter Editions.
[3] Analyse d'images: filtrage et segmentation, J.P. Cocquerez, S. Philippe, Masson.
[4] Evolution d'entités virtuelles coopératives par système de classifieurs, C. Sanza Thèse de doctorat, Université Paul Sabatier, Toulouse, juin 2001.
[5] Reconnaissance et contexte : une approche coopérative pour la lecture de textes imprimés, J.L. Henry Thèse de doctorat, institut des sciences appliquées de Lyon. Lyon, mars 1996.

*Environment / Climate / Natural Hazard / Simulation*

## Initialization of an Atmospheric Mesoscale Model for the Prediction of the Track and Intensity of Hurricanes

W. SICOT

*LPAT, Université des Antilles et de la Guyane, Faculté SEN, Campus de Fouillole, Pointe-à-Pitre, Guadeloupe wsicot@univ-ag.fr*

**Abstract**

A bogus vortex method in order to initialise the Oklahoma University mesoscale model ARPS (Advanced Regional Prediction System) for the prediction of track and intensity of hurricanes on a 24 hours base is presented in this paper. The atmospheric fields issued from the Global Forecasting System (GFS) analysis are used for the model initialization. The approach adopted here consists of modifying the initial GFS pressure analysis field by implementing an axi-symetric pressure distribution. The latter is elaborated by using observed pressure values in the neighbourhood of the eye and the corresponding characteristic cyclonic vortex radii data. The resulting pressure field is used for the ARPS initialization. After a first six hours run (including the model spin-up time), a cyclonic vortex formation is observed. The resulting atmospheric fields are then used in a second run in order to determine the vortex trajectory and corresponding strength during a 24 hour period. In order to test this method, a numerical experiment has been drawn by using the data related to the evolution of hurricane Ivan (2004) from the 07 September 2004 12UTC to 08 September 2004 12 UTC. Starting with an initial minimal pressure equal to 963 hPa, the maximum surface wind value increases up to 185 km/h, thus conferring to the vortex the strength of a category 3 hurricane. The comparison between predicted and observed tracks after a 24 hour simulation leads to an 84 km forecast error. This is roughly 8% lower than the 95 km error associated to the NCEP (National Center for Environmental Prediction) prediction for the same time laps.

## Climatology of African Dust using Meteosat IR throughout the Period 1984-1998

M. LEGRAND, O. PANCRATI, N. J. BROOKS AND L. J. SHIPMAN

*Michel Legrand and Ovidiu Pancrati (LOA, Université de Lille-1, 59655 Villeneuve d'Ascq cedex, France). legrand@loa.univ-lille1.fr - ovidiu@loa.univ-lille1.fr*
*J. Brooks and Lisa J. Shipman (CRU, School of Environmental Sciences, University of East Anglia, Norwich NR4 7TJ, U.K.). n.brooks@uea.ac.uk - l.shipman@uea.ac.uk*

**Abstract**

The infrared method enables the monitoring of the desert aerosol plumes over the African continent (and the Middle East), using Meteosat observations of the middle of the day. The method is based on the strong dust forcing in the thermal IR, involving the additive effects of the radiative cooling of the ground surface and of the upward infrared radiance extinction through the dust layer. Remote sensing of dust plumes is achieved through an algorithm operating on the Meteosat IR imagery. As a result, daily images of Infrared Difference Dust Index (IDDI) are obtained. The method is applied to the series of B2-ISCCP-formatted images covering the period 1984-1998. The resulting dataset constitutes the basis of a climatology 15-year long of the Saharan, Sahelian, Somalian, Arabian and South African dust events. Such a climatology consists of monthly means of IDDI (brightness temperature) and monthly frequencies of dust occurrence, computed for 1° square pixels. The dust distribution is observed to obey a marked annual cycle alternating turbid and comparatively cleaner periods. The year-to-year variability as well as the long term trend are analysed. The sources of dust emission are identified and their seasonal cycle of activity is described.

*Environment / Climate / Natural Hazard / Simulation*

## Evaluation of Rainfall Over Guadeloupe by Four Cumulus Parameterization Schemes: Case of the Tropical Depression Jeanne

C. JEAN-CHARLES, ASSELIN DE BEAUVILLE

*Université des Antilles et de la Guyane, faculté des sciences, Laboratoire de Physique de l'Atmosphère LPAT-GEOLBP250 - 97157 Pointe-à-Pitre cedex, Guadeloupe - cedric.jean-charles@univ-ag.fr*

**Abstract**

Evaluation of rainfall over Guadeloupe by four cumulus parameterization schemes:
Case of the tropical depression Jeanne.

As it approaches the Lesser Antilles, a tropical wave presents signs of organization. It becomes a tropical depression (n 11) on Monday, September 13, 2004 at the end of the afternoon. The centre of the depression passes over Guadeloupe in the course of the night (minimal atmospheric pressure: 1009.1 hPa at 02. 03 local time). The continuous precipitations increase a lot during the night and storms burst out on the coast down-wind of the island of Basse-Terre. Very important rain intensities are observed in this region.

The frame of this study is the forecast of precipitation in the case of a cyclonic phenomenon, with great potential precipitation, during the warm season. We compare the results of precipitation simulations of this phenomenon obtained by using four different cumulus parameterization schemes in ARPS (Advanced Regional Prevision System), a meso-scale model of atmospheric forecast. The four schemes are: Kuo and Kessler's warm rain microphysics, Kaint and Fritsch's cumulus parameterization, Betts-Miller-Janjic's cumulus parameterization and finally the new Kaint-Fritsch's scheme (1994). The model has a 2 km grid resolution because of the exiguous character of the Guadeloupe archipelago and the variability of the relief. We initialize the model (already containing the vortex that represents the depression) with data from the AVN global file corresponding to September 13, 2004 at 00 hr UT and make 24 hour simulations. The precipitation obtained with the model and its different parameterizations is then compared to the maximum observed values, throughout the island's rain gauge network.

The parameterization of Kuo and Kessler overestimates the quantities of fallen precipitation but represents quite well the major part of the flooded zones. The other parameterizations underestimate the quantities of precipitation, whether it is in the accumulated value or the hourly one, and have trouble in representing effectively the zones of strong precipitation. Our results are in good agreement with Yang and Tung's (2003) results, for whom the Kaint-Fritsch and Betts-Miller schemes gave interesting results for the cold season events but underestimated the precipitation values for the warm season.

## Estimation of Downward Longwave Radiation in Guadeloupe

A. FOUERE, R. BONHOMME, F. BUSIERE AND S. DUFOUR-KOWALSKYS

*Unité APC, INRA, Domaine Duclos, 97170 Petit-Bourg, Guadeloupe, France*
*Alain.Fouere@antilles.inra.fr*

**Abstract**

The downward longwave radiation (Rld), thermal infrared radiation emitted by atmospheric constituents is a main component of the radiative budget at the soil surface. The estimation of Rld is required in many domains of human activity like energy management for buildings or natural environment or in climate modelling. An accurate estimate of Rld is particularly required in agronomy and forestry sciences for the estimation of soil and plant canopies temperature and evaporation.

However measurements of Rld are quite rare in temperate countries and nearly inexistent in the humid tropics because of the cost of the sensors and the complex routine operation required by these radiometers.

We measured hourly Rld in Guadeloupe over several months with an Eppley pyrgeometer, a radiative sensor using a KRS 5 filter that is transparent to thermal infrared radiation and was periodically carefully calibrated with a black body emitter

The mean annual downward long wave radiation in Guadeloupe was high in comparison to existing estimates in temperate continental situations (412 ± 19 Wm-2). Such fluxes prevent night radiative cooling and explains the rather high nocturnal minimal temperatures observed in humid tropics. The lowest Rld measured in our conditions were about 350 Wm-2, that corresponded to a 7°C radiative sky temperature. This lowest sky temperature was high when compared to negative sky temperature classically recorded during clear nights in temperate latitudes. The daily and annual variability of our measurements for three years was only 100 Wm-2. This variability was low in comparison with the range 162-250 found in published large data series. These Rld behaviour confirmed the great influence of the constant high water content of the tropical atmosphere.
We then discussed the influences of air temperature and atmospheric vapour pressure in order to propose empirical formulae for tropical Rld estimate.

## Early Observations of the Blazar OJ 287: Further Evidence for the Binary Black Hole Model

H. RAMPADARATH (1) , M.J. VALTONEN (2), R. SAUNDERS (1) and H.J. LEHTO (1)

*(1) Physics Department, University of the West Indies, St. Augustine Campus, Trinidad*
*rsaunders@fsa.uwi.tt*
*(2) Tuorla Observatory, Turku University, Piikkiö, Finland*

**Abstract**

OJ 287 is one of the most active blazars, and with an optical light curve covering over 100 years, it is the most observed. The observations after 1972 are quite dense, from which the optical behaviour is clear, but prior to 1972 data are scarce. These data are of great scientific value, as there are hints for the periodicity in the historical light curve, which could be used to definitely confirm the binary black hole nature of this object. In this study, the optical behaviour of OJ 287 during the years 1957-1965 was analyzed using digitally scanned photographic plates. Given that photographic plates are non-linear detectors, each scanned plate must be individually calibrated. The method of analysis was adapted from Innis et al (2004), in which a transformation equation relating instrumental magnitudes, Mi and B magnitude was derived for each plate. The method employed aperture photometry to obtain Mi, and the singular value decomposition (SVD) least squares method (Press et al 1992) to determine the calibration equations.
The new data collected from the scanned plates, were plotted with the previous data. This time period provides a unique study, since there are three disc crossings very close; 1956, 1959 and 1963, with a tidal outburst in 1960. The results show evidence that a disc impact outburst occurred around 1963.31-1963.41. The results favor the 'active disc' model of Sundelius et al (1997), which predicts the outburst to occur in 1963.21. In this model, the accretion disc of the primary black hole moves to meet the incoming secondary black hole causing the impact to occur earlier, this is shown by the results of this study. The predicted time of the 1963 outburst without the active disc is given by the Lehto and Valtonen (1996) binary black hole model, as 1963.59. The time of the 1963 outburst is approximately 4.1 yrs after the primary impact in 1959.2, the other well observed outbursts' secondary follows within 1-2 years. This result supports the precessing orbit of the binary black hole models of both Lehto and Valtonen (1996) and Sundelius et al (1997).

**References**

Lehto H.J., and Valtonen M.J. 1996. OJ 287 Outburst Structure and a Binary Black Hole Model. The Astrophysical Journal 460, 207-213
Sundelius B., Wahde M., Lehto H.J., and Valtonen M.J. 1997. A Numerical Simulation of the Brightness Variations of OJ 287. The Astrophysical Journal 484, 180-185
Innis J.L., Borisova A.P., Coates D.W., and Tsvetkov M.K. 2004. Archival lightcurves from the Bamberg Sky Patrol; CF Octantis, 1964 – 76.
Press W.H., Teukolsky S.A., Vetterling W.T., Flannery B.P., 1992 Numerical Recipies in Fortran. Cambridge University Press, Cambridge